Mechanistic macroecology: exploring the drivers of latitudinal variation in terrestrial body size in a General Ecosystem Model

RUNNING TITLE: Mechanistic macroecology in a GEM

KEYWORDS: Bergmann's rule, Mechanistic macroecology, General Ecosystem Model, Madingley, thermoregulation, resource availability, body mass, body size, mechanism.

ABSTRACT

Many mechanisms have been hypothesized to explain Bergmann's rule - the correlation of body size with latitude. However, it is not feasible to assess the contribution of hypothesised mechanisms by experimental manipulation or statistical correlation. Here, we evaluate two of the principal hypothesised mechanisms, related to thermoregulation and resource availability, using structured experiments in a mechanistic global ecosystem model. We simulated the broad structure of assemblages and ecosystems using the Madingley model, a mechanistic General Ecosystem Model (GEM). We compared emergent modelled biogeographic patterns in body mass to empirical patterns for mammals and birds. We then explored the relative contribution of thermoregulation and resource availability to body mass clines by manipulating the model's environmental gradients. Madingley produces body size gradients that are in broad agreement with empirically estimates. Thermoregulation and resource availability were both important controls on body mass for endotherms, but only temperature for ectotherms. Our results suggest that seasonality explains animal body mass patterns through a complex set of mechanisms. Process-based GEMs generate broadly realistic biogeographic body mass patterns. Ecologists can use them in novel ways: to explore causality, or for generating and testing hypotheses for large-scale, emergent ecological patterns. At the same time,

macroecological patterns are useful for evaluating mechanistic models. Iteratively developing GEMs, and evaluating them against macroecological patterns, could generate new insights into the complex causes of such patterns.

INTRODUCTION

The role of mechanistic models in macroecology

The fields of macroecology and biogeography have traditionally adopted a strong observational and descriptive approach to understanding patterns of species distributions, community composition and biodiversity across space and time (Blackburn et al., 1999). Correlative, statistical approaches have been the primary tools for exploring such data but they are unable to establish causal relationships and can be difficult to transfer across geographic space, time and environmental space (Cabral et al., 2017). Mechanistic ecological models are a new approach that can complement such studies. They represent both the composition of ecosystems and the causal relationships determining that composition. So, they permit targeted exploration of causality in macroecology (Connolly et al., 2017), especially at the large scales are which experimental manipulation is not possible.

Latitudinal variation in body size and the hypothesised mechanisms

Bergmann's rule, one of the oldest macroecological patterns (Bergmann, 1847), hypothesises that size is positively correlated with latitude and elevation, with heat conservation increased in larger-bodied animals through a smaller surface-area-to-volume ratio (James 1970, Blackburn et al., 1999). Bergmann's rule can be considered an empirical generalisation (Mayr, 1956, Meiri, 2011) and has been applied in both inter- and intra-specific studies to a broad range of taxa, including ectotherms, in multiple geographic regions. Amongst endotherms, the majority of mammal and bird species appear to exhibit Bergmann clines (Ashton, 2002; Cardillo, 2002; Freckleton et al., 2003; Meiri et al., 2004; Rodriguez et al., 2006; Ramirez et al.,

2008; Rodríguez et al., 2008; Olson et al., 2009; Morales-Castilla et al. 2012a,b; Torres-Romero et al. 2016), though converse clines exist, for example in a group of subterranean rodents (Medina et al., 2007). In contrast, the evidence for ectotherms is highly ambiguous. Some ectothermic taxa conform well (Olalla-Tárraga and Rodríguez, 2007), whilst others show inverse clines (Mosseau, 1997; Ashton and Feldmann, 2003; Olalla-Tárraga and Rodríguez, 2007; Adams and Church, 2008; Cvetkovic et al., 2009) and some show no pattern at all (Olalla-Tárraga et al., 2006; Pincheria-Donoso and Meiri, 2013; Feldman and Meiri, 2014, Slavenko et al. 2019). Despite over 170 years of scientific research, both the generality and the underlying mechanism(s) of this ecogeographic rule thus remain disputed (James, 1970; Blackburn et al., 1999; Meiri and Dayan, 2003; Pincheria-Donoso, 2010; Meiri, 2011).

Multiple mechanisms have been proposed to explain the observed patterns in body mass for both endotherms and ectotherms (Blackburn et al., 1999; Olalla-Tárraga, 2011) (Table 1). Here we describe two leading mechanisms hypothesised to determine body size clines, which will be the focus of this study.

First, Bergmann's original hypothesis relates to endotherms and suggests a thermoregulatory mechanism, proposing that larger organisms conserve heat more effectively in cooler environments, by virtue of their lower surface area to volume ratio, compared to smaller organisms. So, a larger body size is an adaptation to cold because larger endotherms expend less energy per unit mass with decreasing temperature compared with smaller endotherms. Others have demonstrated that environmental seasonality can have a strong selection effects on life history selection including body size because it influences both the availability the essential resources and the ability of organisms to access them, for example by limiting an organism's diurnal activity (Lindsay, 1966; Boyce, 1979). For ectotherms, it has been proposed that evidence for converse Bergmann clines in ectotherms can be explained by the ability of smaller ectotherms to more effectively use limited benign environmental conditions in cold environments relative to larger ectotherms. This hypothesis would select for smaller sized ectotherms in high latitudes (Ashton and Feldmann, 2003; Olalla-Tárraga and Rodríguez, 2007)

The second mechanism relates to resource availability, which has been linked to several hypotheses. Rosenweig (1968) argued that maintenance of a particular body mass depends on a sufficient supply of food resources and to meet physiological demands, larger bodied species require more resources. He proposed that the net primary productivity of terrestrial communities increases with latitude, permitting larger size with latitude. Giest (1987) argued that the increase in primary production with latitude permits the body sizes of herbivores to increase and consequently, the body size of their dependent carnivores. Further hypotheses have proposed that the seasonal variation of resources and in particular the amount of resources available during the reproduction and growing periods is critical for determining the body size that can be supported (McNab, 2010; Wolverton et al., 2009; Huston and Wolverton, 2011). Others, such as Lyndsay (1966) and Boyce (1979) proposed that increased seasonality of resource availability drives larger body sizes because large organisms are better able to resist longer period of little food because they have relatively more fat deposits and deplete them more slowly.

Aims of this study

In reality, it is likely that the observed clines arise from interactions between several of these mechanisms (Mayr 1956). But one of the key challenges in resolving causes of observed biogeographic patterns in animal body mass has been difficulty in modelling them at regional and global scales. Although statistical modelling of empirical data is feasible, it is not an approach that can be used to resolve underlying mechanisms (i.e., correlation may not imply causality; Gaston, 2000; Marquet et al., 2014; Cabral et al., 2017). Alternative approaches that explicitly incorporate such mechanisms are required. Doing so experimentally at global scales is infeasible, and hence using models based on underlying ecosystem theory and performing systematic, ‘knock out’ experiments to test the importance of individual mechanisms is a promising, if underexplored, approach. It is made possible by the recent development of general ecosystem models (GEMs; Purves et al., 2013), based on fundamental ecological principles, and allowing self-assembling ecosystems to generate emergent patterns - that can be assessed against empirical data.

Here we explore the thermoregulation and resource availability mechanisms hypothesised to be responsible for latitudinal variation in endotherm body size. We apply a series of structured simulation experiments using the Madingley General Ecosystem Model (GEM), a global, virtual ecological world based on prominent ecological theories (Harfoot et al. 2014). In these simulations, macroecological patterns are entirely emergent, bottom-up, from ecological principles encoded within the Madingley model at the individual level. Therefore, we begin by evaluating the modelled biogeographic patterns in animal body mass against empirically derived patterns to demonstrate that the model can generate body size gradients that are comparable to those estimated empirically. We focus on evaluating endotherm patterns because the evidence for latitudinal body size gradients in endotherms is much stronger than for ectotherms. Subsequently, to explore the relative importance of the thermoregulation and resource availability hypotheses in driving biogeographic patterns in terrestrial animal body mass, we isolate and manipulate the model's environmental gradients in absolute and seasonality of temperature and productivity, and examine their effects on modelled animal assemblages.

MATERIALS AND METHODS

The Madingley General Ecosystem Model

The Madingley model is a mechanistic and individual-based model of whole ecosystems. It was developed with the twin aims of synthesizing and advancing our understanding of ecology, and of enabling mechanistic prediction of the structure and function of whole ecosystems at various levels of organisation. Madingley encodes a prominent ecological theories that govern the metabolism, feeding, reproduction, movement and mortality. It is general in the sense that it applies these same functions to all organisms in all ecosystems and individual-based because the functions are specified at the level of individual organisms.

Pertinent components

A comprehensive description of the model is provided by Harfoot et al (2014). Here we summarise the model's pertinent components, which simulate the dynamics of plants, and all heterotrophs with body masses above 4×10^{-4}g that feed on living organisms. Organisms are not characterised by species identity and are instead grouped according to a set of categorical functional traits - for example trophic level (herbivores, omnivores and carnivores), reproductive strategy (semelparity vs. iteroparity), thermoregulatory mode (endothermy vs. ectothermy), and mobility for animals. These traits determine the types of ecological interactions that modelled organisms are involved in, whilst a set of continuous traits - total biomass of autotrophs; and current body mass, juvenile body mass, adult body mass, and optimal prey size of omnivorous and carnivorous heterotrophs - determine the rates of each process.

Plants

On land, plants are represented by stocks, or pools, of biomass modelled using a terrestrial carbon model. Biomass is added to the stocks though the process of primary production, the seasonality of which is calculated using remotely sensed Net Primary Productivity data (Harfoot et al., 2014). This production is allocated to above-ground/below-ground, structural/non-structural, evergreen/deciduous components. The Madingley model assumes that all above-ground, non-structural, matter is available for heterotrophic organisms to consume. Biomass is lost from plant stocks through mortality from fire and senescence, as well as through herbivory, which is described in more detail below. Production, allocation and mortality, in the plant model, are all determined by environmental conditions (temperature, number of frost days, precipitation, and the available water capacity of soils) (Smith et al., 2013).

Animals

Heterotrophic animals are represented in the model as 'cohorts', the fundamental agents of the model: collections of individual organisms occurring in the same modelled grid cell and that follow the same

ecological trajectory, with identical categorical and continuous functional traits. Representing individual organisms is of course computationally unfeasible - there are simply too many individual organisms on Earth - but the cohort approach enables the model to predict emergent ecosystem properties at organisational scales from individuals to the whole ecosystem. Heterotroph dynamics result from five ecological processes: metabolism, eating, reproduction, mortality and dispersal (see Text S1 and Figure S1). The model can be considered as an ecological null model. It is intended to describe broad patterns, and hence does not include all ecological processes, such as, for example, ecological stoichiometry, behaviour (e.g. predator avoidance, sociality and intelligent movement) or microhabitat use. The model currently does not resolve flying organisms explicitly and so is more representative of non-volant organisms.

All endothermic functional groups in the model were iteroparous and initially seeded cohorts ranged between 1.5g as the smallest juvenile mass and 5×10^{6}g as the largest herbivorous endotherm adult (7×10^{5}g for carnivorous endotherms, 1.5×10^{6}g for omnivorous endotherms). Also endothermic cohorts are assumed to thermoregulate at 37°C at all times and that this thermoregulation comes at no extra metabolic costs. Ectotherms were either iteroparous or semelparous. Cohorts were initially seeded into the model ranging between 4×10^{-4}g as the smallest juvenile mass and 2×10^{6}g as the largest adult mass depending on the functional group. Ectotherm activity was limited by environmental conditions according to the empirically relationships between activity, diurnal temperature ranges, annual mean temperature and annual variation (Sunday et al., 2010). After the initial quasi-random seeding, cohorts interact with each other and with plant stocks, influenced by the environment, to select for a dynamic equilibrium ecosystem composition.

Resolution

The model is flexible with regard to spatial and temporal resolution. As described below we used two spatial resolutions one at 1° x 1°, to compare the model with empirical patterns, and the other at 5° x 5° for the set of knockout simulations. The coarser resolution was employed for computational efficiency given the 40 model simulations required for the knockout experiments, and as in the original formulation (Harfoot et al.,

2014), we used a monthly time step throughout. We modelled the terrestrial realm exclusively, as this realm has seen the most research into empirical Bergmann clines (though see Torres-Romero et al., 2016). Comparisons to marine patterns would make an interesting further exploration. We simulated ecosystem structure for all terrestrial landmass between 65°N to 65°S in latitude.

Evaluating emergent biogeographic patterns in body size

The Madingley model has previously been demonstrated to capture observed properties of individual organisms and the coarse structure of ecosystems reasonably well under environmental conditions without human impact (Harfoot et al., 2014). To explore latitudinal patterns in animal body mass, we used emergent ecosystem structure in the global grid of 1° × 1° terrestrial cells. Climatological environmental conditions for each grid-cell are read as model inputs from publicly-available datasets (see Harfoot et al., 2014). For air temperature, diurnal temperature range, precipitation and number of frost days these were calculated from WorldClim mid-Holocene (approximately 6,000 years ago) downscaling of the HadGEM2-ES model reconstruction (Hijmans et al., 2005), while soil water availability values were averages over the period 1960 - 2000. We used the same climatological time series for each of the 100 years of model simulations, to remove the effects of inter-annual environmental variation. Importantly, we also excluded effects of anthropogenic habitat conversion and harvesting of plant or animal biomass for human use. So our simulations represent a late-Quaternary world that has received little anthropogenic influence.

We performed 10 simulations with this protocol, in each case drawing different initial ecosystem states to capture the effects of variation in initial conditions and of stochasticity in ecological dynamics, and allowing the ecosystems to establish a quasi-steady state over a simulation length of 100 years. Figure S2 shows the temporal emergence of body mass gradients over the 100 year period. It demonstrates that there is no body-mass cline associated with initial conditions. The final heterotroph biogeography is instead determined by the environmental and productivity conditions in each grid cell.

To be consistent with the empirical body size gradients (described below), which do not take abundance into account, and use species maximum or adult body mass, we grouped cohorts (which represent functionally equivalent, hetero-specific individuals, at a specific life stage) by their unique adult body mass, creating pseudo-species. For each grid cell and each simulation we calculated the annual mean of the median adult body mass of the pseudo-species. We calculated this using the quasi-steady state ecosystems of the final 12 months of each simulation. We used the most central simulation from the ensemble to calculate these body size biogeography. The central ensemble member was the simulation with the minimum sum-squared error in mean body size across grid cells, compared to all other ensemble members.

Estimating empirical biogeographic patterns of animal body mass

Estimates of the community mean body mass for mammals and birds were derived from extent of occurrence maps (EOO) and trait databases. We refer to these data as mean body mass from EOO. Extents of occurrence were intersected with the same 1° × 1° grid of cells used for the model simulations. For the species occurring in each grid cell, the median assemblage body mass was calculated (Cooper & Purvis, 2010; Rapacciuolo et al., 2017).

As introduced above, we focus our evaluation of modelled biogeographic body mass patterns on endotherms, where there is much stronger evidence of latitudinal body mass clines, however see Supplementary Text S2 for further information about comparison of modelled and empirical datasets, as well as for ectotherm patterns. For mammals, where there is evidence that anthropogenic impacts have altered the latitudinal gradients in body mass (Faurby & Araújo, 2016; Santini et al., 2017b). We used Holocene body mass data and present-natural EOO for 5,706 terrestrial mammal species (Faurby and Svenning 2015). These estimate what the present range would be for each mammal species if there had been no human impacts. Mammal EOO data are available from http://bios.au.dk/en/about-bioscience/organisation/ecoinformatics-and-biodiversity/data/). The Holocene EOO maps were projected

in the Behrmann equal area coordinate system so the maps were sampled at the coordinates of the 1 decimal degree model grid cell centres projected to Behrmann coordinate system. Further details can be found in Supplementary Text S2.

For birds historic range maps are not available. So present day EOO maps were taken from the IUCN Red List (BirdLife International & NatureServe, 2017; IUCN, 2017). We used resident and breeding ranges within the EOO maps. This approach is supported by the limited evidence for human impact on latitudinal gradients in body mass (Rapacciolo et al., 2017). We extracted body masses for 9,993 bird species from Elton Traits v 1.0 (Wilman et al., 2014).

Evaluating modelled biogeographic patterns of animal body mass

We evaluated emergent body mass patterns by calculating their correlation with empirical estimates across the global grid using modified t-tests to account for the loss of statistical power resulting from spatial autocorrelation (Dormann et al., 2007; Dutilleul et al., 2008). We log transformed body masses to give equal weight in the correlation to all body sizes across the orders of magnitude variation in sizes across the grid. We did not take phylogenetic correlation into account because Madingley does not contain phylogenetic information.

Isolating mechanisms driving body-mass patterns

Thermoregulation and resource availability hypotheses

We conducted a set of environmental knockout simulation experiments in the model to investigate the two major hypothesised environmental drivers of clines in body mass: thermoregulation and resource availability. We considered two aspects of the thermoregulatory hypothesis: that the latitudinal gradients in annual mean temperature or the variation in temperature through the year (seasonality of temperature), selects for larger endotherms where either annual mean or seasonality of temperature is higher. We also considered whether these conditions select for smaller ectotherms, through their capacity to more

effectively utilise benign windows in otherwise unsuitable environments (e.g. Olalla-Tárraga and Rodríguez, 2007). Analogously to the temperature knockout simulations, we tested for the effects of latitudinal gradients in the cumulative annual net primary production and the variation in net primary productivity through the year (seasonality of production). Our prediction was that higher annual mean productivity and greater seasonality of production selects for larger endotherms (Lindsey 1966, Rosenweig, 1968, Boyce 1978, 1979). We therefore conducted, in addition to a control, or full, simulation with no environment changed, four knockout experiments in each of which we removed either a gradient or variation in one of these aspect of the environment at a time (Table 1, Fig S3). These knockout simulations were then compared to the full simulations.

Experimental protocol

To account for stochastic effects, we performed an ensemble of 10 simulations for the control conditions and for each knockout, which yielded 50 simulation runs. It was computationally unfeasible to run these simulations at a resolution of 1° × 1°, so we used a coarser resolution of 5° × 5° cells with the same extent. The change in resolution did not substantially alter the emergent body mass patterns across latitude. For each knockout experiment, we calculated the central member of the ensemble, following the same methods described above. For each knockout across each latitude band, we then calculated the relative median body mass deviation from the unmodified control simulation.

Exploring causation

To further explore the causes of changes in latitudinal body mass clines in response to environmental knockouts, we analysed changes in individual level feeding, reproduction and mortality rates. We ran simulations for two grids of four 5° × 5° cells, one in North Asia (55-65°N and 75-85°E) and one in equatorial Africa (5°S-5°N and 5-15°E). These grids were representative of different environments and exhibited analogous patterns to the global simulation when run outside the global model. These simulations were run for 20 years and for each month we exported the process rates (feeding/assimilation, reproductive

output, per capita mortality) of every cohort as well as cohort properties (e.g. current body mass, adult mass and cohort abundance). It was not possible to run a global simulation because of the prohibitively long runtimes and large volumes of individual level ecological data generated. Annual rates of the ecological processes were calculated for each individual within each cohort by summing the monthly outputs. See Text S3 for further methodological details.

RESULTS

Global patterns of modelled animal body mass

Spatial patterns of endotherm and ectotherm body mass emerge from the model without exogenous constraints based on its parsimonious descriptions of the ecological processes governing ecosystem structure and function (Figure S2). These patterns exhibit strong spatial and latitudinal variation (Figure 1). For endotherms, median body mass generally increases with aridity and with latitude (Figure 1a), whilst ectotherms display a negative relationships between body mass and increasing absolute latitude (Supplementary Figure S4) but with evidence that median body mass increases with aridity (e.g. central and western Australia).

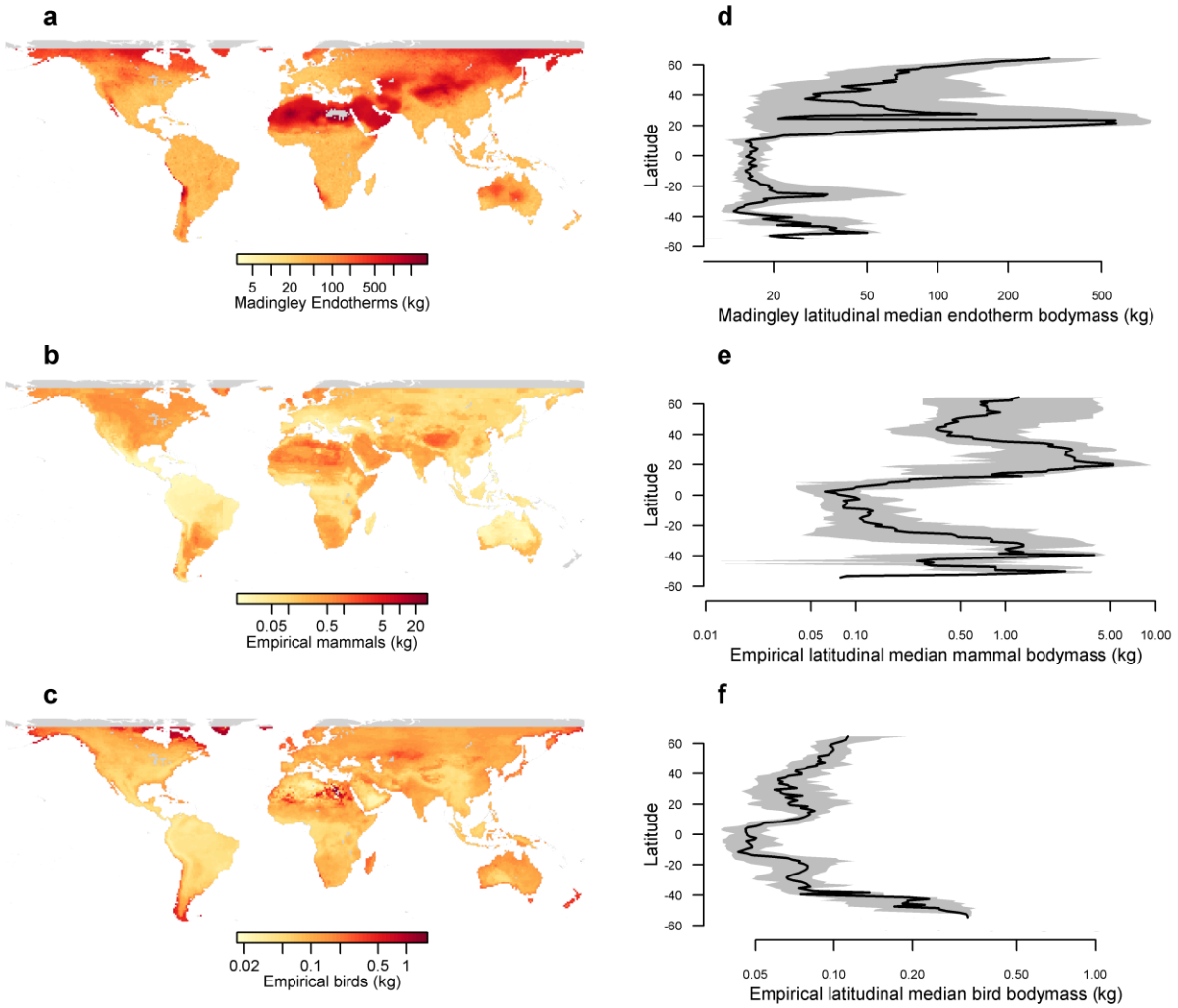

Figure 1. Global distributions (a-c) and latitudinal profiles (d-f) of annual mean, community median body masses of endotherms predicted by the Madingley model (a, d), Holocene mammals estimated from empirical data (b, e), present-day birds estimated from empirical data (c, f).

Comparing modelled and empirical body mass

Endotherms

Endotherms (i.e., birds and mammals) modelled by Madingley exhibit spatial variation in body mass that resembles empirical patterns (Figure 1a-c). Modelled body sizes increased in northern USA and Canada, south west Africa, the Sahara, and central Asia consistent with empirical patterns in mammals. Modelled and empirical body sizes were significantly, positively correlated at the global scale (Mammals: r = 0.37,

$p < 1\times10^{-5}$, modified t-test; Birds $r = 0.31$, $p < 1\times10^{-5}$, modified t-test). Central and western Australia stands out as showing disagreement. Here, Madingley suggests larger body masses than the east coast of Australia, whilst the empirical data for mammals and birds suggests the opposite. Although modelled and empirical body masses are correlated, in general, the organisms predicted by Madingley were much larger than those estimated from empirical data by about two orders of magnitude.

Latitudinal profiles show that Madingley predicts Bergmann-like clines that are similar in shape to those for Holocene mammals and for present day birds (Figure 1d-f). Body masses are at their lowest in the sub-tropics. They increase towards the highest latitudes but with peaks around the desert belt.

Knockout experiments

Environmental knockouts

We found support for the resource availability drivers of body mass clines. When the latitudinal gradient in NPP was removed (NPP-flat, Table 2), endotherm body masses consistently declined significantly (negative proportional body mass deviation, with 95% interval below zero) across the Northern hemisphere. When we removed variation in NPP across the year (NPP-aseasonal), body masses declined significantly in high latitudes in both hemispheres. For both NPP-flat and NPP-aseasonal, changes were of smaller magnitude and less frequently significant in tropical latitudes. In both these environmental knockouts, the latitudinal median of the grid-cell median adult endotherm body mass was reduced (median declines of 67% for NPP-flat, 52% for NPP-aseasonal, and 62% for T-aseasonal; Figure 2). In the southern hemisphere, NPP-aseasonal and T-aseasonal knockout simulations generally resulted in lower community-mean endotherm body mass across most latitudes, with the NPP-aseasonal knockout simulation causing a median body mass decline of 35% and T-aseasonal resulting in a median decline of 18% decline. NPP-flat resulted in a variable response across latitudes, sometimes endotherm body mass increased and sometimes decreased. T-flat had no consistent effect on endotherm body mass in the northern hemisphere but tended to result in larger organisms across most south hemisphere latitudes.

The ectotherm responses to knockouts provided support for the seasonality aspect of both the thermoregulation and resource availability drivers. Median ectotherm body mass was more variable across latitudes than that for endotherms and relative mass changes were also larger (Figure 2). When there was no seasonal variation in T, and so no limitation on ectotherm activity (T-aseasonal), there was a substantial and significant increase in body mass across latitudes above 32.5°N (median of 190%) and between -32.5°S and 47.5°S (median 30%). NPP-aseasonal resulted in body mass decline across most latitudes, analogous to the endothermic response but the ectotherms exhibited more variability across longitudes.

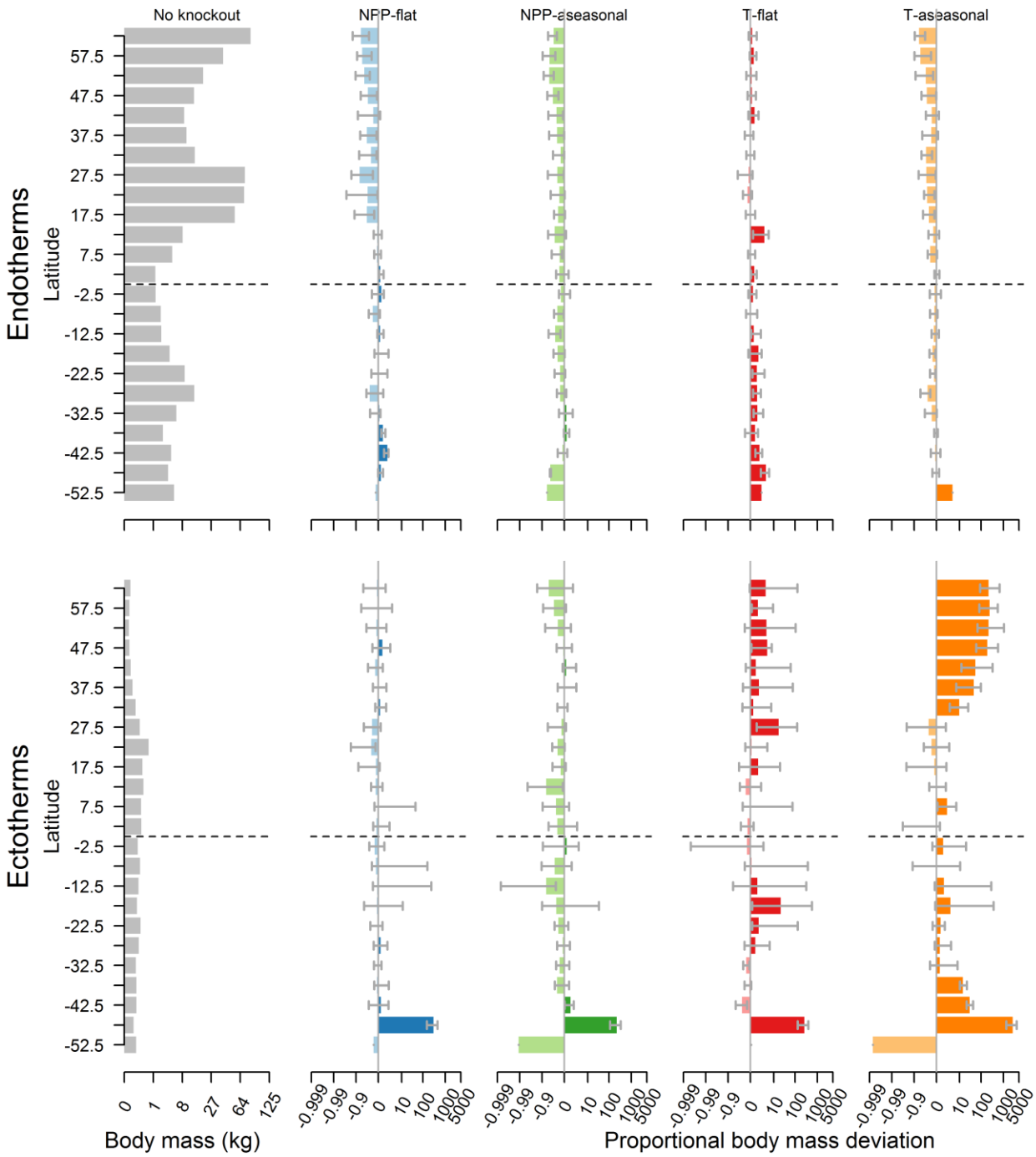

Figure 2. The relative effect on community mean endotherm and ectotherm body mass across latitudes of removing spatial variation in cumulative annual primary production, seasonality of primary production, annual mean temperature and annual temperature seasonality. Solid bars represent the median and grey

lines the interquartile range across longitudes with each latitude band. Lighter hue indicates negative median effect whilst darker indicates a positive median effect

Exploring causation: Individual level ecological responses

The results from a grid cell in North Asia (central Russia, 62.5°N, 82.5°E) showed that, for endotherms, in all knockouts other than T-flat, median body masses declined because smaller organisms persisted in the model (Figure 3a). NPP-aseasonal had the largest effect followed by T-aseasonal. In terms of differential effects on organisms of different body mass, smaller organisms tended to assimilate more biomass, produce more offspring and have lower starvation mortality losses relative to the full environment for all knockouts except T-flat (Figure 3b, S5).

For ectotherms, median body mass increased in all knockout simulations except the NPP-flat (Figure 4). The largest effects arose in the T-flat and T-aseasonal simulations. T-flat resulted in ectotherms with body mass less than 10g dying out, and orders of magnitude lower abundances of larger ectotherms. This arose because the interaction of warmer temperatures but with retained seasonality patterns reduced the period of the year in which ectotherms were active in the model. As a result, the likelihoods and rates of assimilation and reproduction were reduced and rates of starvation mortality were substantially elevated, especially for smaller ectotherms with a higher relative metabolic rate. T-aseasonal resulted in decreased abundance of the smallest, and an increase in the abundance of the largest, ectotherms. Ectotherms in this experiment were active all year round in the model (there was no unsuitable winter season) hence the probabilities and rates of assimilating or reproducing raised and reproductive output was increased, especially for smaller organisms.

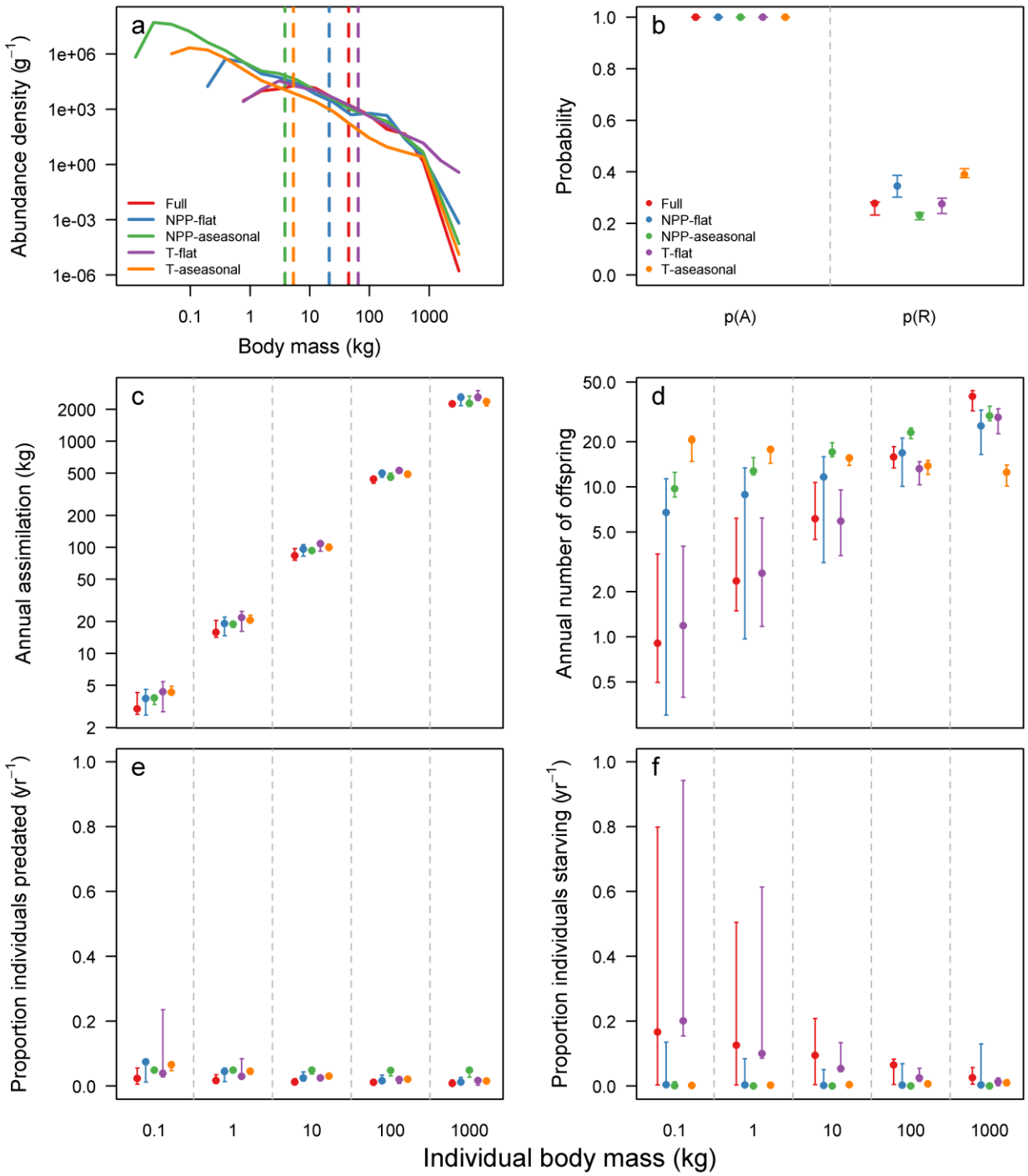

Figure 3. Effect of environmental knockouts in a grid cell centred at 62.5°N and 82.5°E on (a) endotherm community size distribution, (b) probability of assimilating biomass, p(A), and of reproducing offspring, p(R), within a year, (c) annual mass assimilated, (d) number of offspring produced per individual present

at the start of the year, and proportion of individuals present at the start of the year that die from predation (e) or starvation (f) events. The community size distribution is the annual median abundance per mass bin from the 20th year of the simulation, dashed lines indicate the community mean body mass for each knockout. Points in b – f represent median predicted values from models fitted to annual data from the last 5 years of a 20 year simulation, error bars represent maximum and minimum value across years.

The results from environmental knockouts in an equatorial ecosystem (2.5°N and 12.5°E) showed limited changes in the abundance size distribution of endotherms (Figures S6-S8). Conversely, for ectotherms, the median body mass decreased by five orders of magnitude in the T-aseasonal knockout. This was caused by the increased likelihood and rate of reproduction of smaller ectotherms but reduced output of larger ectotherms, compared to the full environment. Smaller ectotherms were also less likely to starve in the aseasonal temperature environment when compared to the full environment.

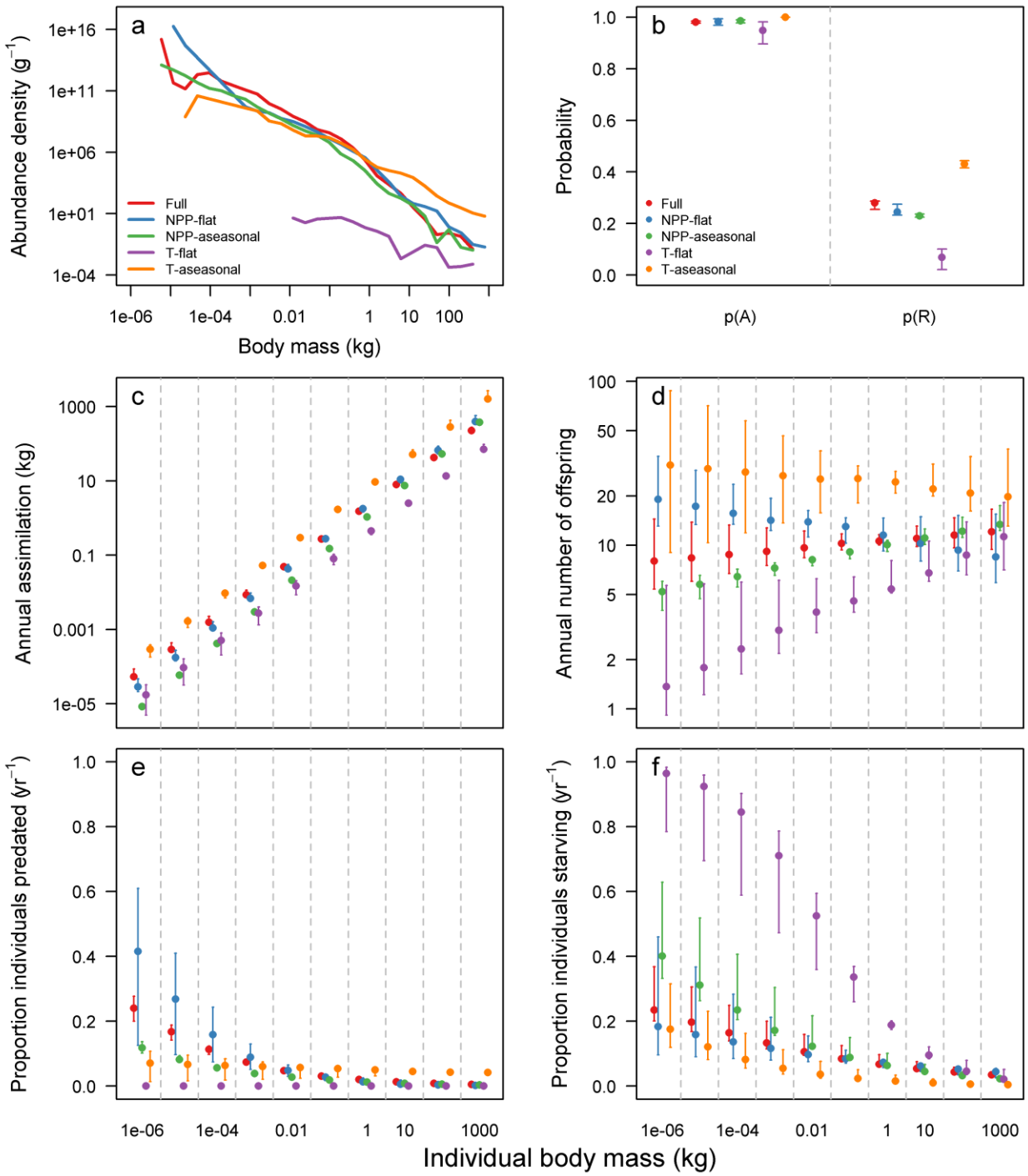

Figure 4. Effect of environmental knockouts in a grid cell centred at 62.5°N and 82.5°E on (a) ectotherm community size distribution, (b) probability of assimilating biomass, p(A), and of reproducing offspring, p(R), within a year, (c) annual mass assimilated, (d) number of offspring produced per individual present

at the start of the year, and proportion of individuals present at the start of the year that die from predation (e) or starvation (f) events. The community size distribution is the annual median abundance per mass bin from the 20th year of the simulation, dashed lines indicate the community mean body mass for each knockout. Points in b – f represent median predicted values from models fitted to annual data from the last 5 years of a 20 year simulation, error bars represent maximum and minimum value across years.

DISCUSSION

Bergmann's rule is an ecological pattern for which there is a complex set of hypothesised mechanisms and varying levels of empirical support. The Madingley model is able to generate global spatial and latitudinal patterns in body mass from individual organismal interactions that are consistent with empirical estimates, while others appear to deviate. Attempting to unpick the variation in body-size attributed to different environmental and ecological drivers provides insight into the potential mechanisms underlying empirical observations. In general, the model captures endothermic patterns reasonably well. Madingley generally over-predicted the body size of organisms compared to empirical estimates. There are several possible factors that might contribute to this disagreement.

First, they represent different things, the median unique adult body masses for all cohorts in a grid cell is not equivalent to the median species size. Because the cohorts in Madingley are hetero-specific, at present the model does not inform about how many species it might represent. A cohort of small endotherms in Madingley might represent many species with small body size. Whilst several cohorts of large organisms in Madingley, might represent intra-specific variation in a single species.

Second, the empirical estimates have substantial associated uncertainties. For example, there can be considerable intraspecific variation in body size across ranges (Ashton, 2002; Clauss et al., 2013; Tseng and Soleimani Pari, 2019). The EOO maps can also contain errors and do not imply that the species is found in every cell within its EOO at all times.

Thirdly, Madingley might be missing mechanisms that limit the maximum size of organisms or increase the survival of smaller organisms. The current formulation of the model misses several aspects of

thermoregulatory behaviour. For example, ectotherms can behaviourally regulate their temperature above or below that of the ambient temperature (Kearney et al., 2009), a process not included in Madingley. So metabolic costs may be under-estimated in cold environments and over-estimated in hot environments. In addition, the model neglects hibernation, and so metabolic costs might be over-estimated in seasonal environments. Including such behaviours could alter the degree of converse Bergmann cline in the model but it is not clear in which direction. The model also currently assumes that thermoregulation in endotherms has a flat metabolic cost across latitudes and that there is no extra metabolic cost associated with, for example, fat deposits, feathers or fur to protect against cold temperatures. Since smaller endotherms pay a greater relative metabolic cost to thermoregulate against extreme temperatures than larger endotherms (Porter and Kearney, 2009), including this effect would likely amplify the latitudinal body mass gradients in the model. As a result of their possibly opposing effects and the complex community assembly processes operating through time, the net impact of including thermoregulatory effects on community body masses is not clear, but should be explored as these features are incorporated into the model.

Nonetheless, our results provide support for the role of both thermoregulation and resource availability mechanisms, and particularly the seasonality of these, as key mechanisms determining body mass of both endotherms and ectotherms.

Despite being hugely simplified in comparison to reality and attempting to model all ecosystems on land at the level of individual organisms, the fundamental ecological mechanisms currently included in the Madingley model produce plausibly realistic emergent geographic pattern of median endotherm body mass. It also captures much of the variation of median body mass within each latitudinal band. For example, desert regions are known as prominent sites of large body mass for birds and mammals (Blackburn and Hawkins, 2004; Olson et al., 2009; Morales-Castilla et al. 2012a), and this is produced by the model outputs. The Saharan and Gobi deserts all harbour greater median animal body mass than the median of their respective latitudes (Figure 1).

We tested hypotheses on the mechanistic factors behind observed patterns through knock-out experiments for environmental factors. The initial conditions of the model are spatially neutral, meaning that there is no initial spatial pattern in the types of cohorts seeded in each grid cell. Therefore, the model does not require chance or mechanisms of migration ability or historical contingencies to generate body mass gradients (see e.g. Morales-Castilla et al. 2012b), implying that while these hypothesised mechanisms may be responsible, Bergmann's clines can be produced without them. There is no *a priori* latitudinal variation in predation risk in the model, therefore this mechanism is also not required for the emergent body mass patterns (Wolverton et al., 2009). Our results suggest that thermoregulation and resource availability are dominant direct controls on endotherm community mean body mass, they as when these factors are removed, or "knocked out", from the model, endotherm body mass across latitudes declines more than for other factors. Where productivity increased or the seasonality of productivity was removed, the severity of the seasonal cycling of food surplus and deficit (sensu Geist, 1987) was reduced, allowing smaller organisms that are more susceptible to starvation, to avoid this risk and increase their fecundity. The resulting abundance increase of smaller endotherms thus draws the community mean body mass down and also exerts some bottom up control over larger endotherms, which have higher starvation rates and lower reproduction rates than the full environment simulations.

For modelled ectotherms, thermoregulation is the dominant control on community body mass through its effect on enabling access to resources. This is because ectotherm activity is limited under extreme ambient temperatures. In simulations that isolated the seasonality of productivity from that of temperature (NPP-aseasonal vs T-aseasonal), the altered seasonal cycling of food surplus and deficit appears unimportant if the temperature remains seasonal such that the organism's ability to use those resources is impeded.

General Ecosystem Models, such as the Madingley model, can generate 'in-silico' global ecosystems that can be experimentally manipulated in ways that are impossible in the real world – allowing for novel

explorations in 'mechanistic macroecology'. Our study demonstrates this for Bergmann's rule, and provides support for the thermoregulation and resource availability hypotheses, while also generating an entirely new hypothesis of trophic interactions between ectotherms and endotherms as a potential structuring mechanism for observed clines in endotherm body mass. While modelled ectotherm clines do not show Bergmann's patterns, empirical data and previous studies are themselves equivocal and show inconsistencies among taxa. While 'mechanistic macroecology' cannot be the only solution or approach to unpicking global macroecological patterns, our study suggests that it is a tool that should be investigated further beyond these preliminary explorations, and can provide both ecological insight and identify model weaknesses or missing processes. Furthermore, our finding that bottom up control of endotherm body mass by ectotherms suggest that we must model ecosystems and biological interactions holistically to better capture how they are structured and function.

REFERENCES

Adams, D.C. and Church, O.C. (2008) Amphibians do not follow Bergmann's rule. *The Society for the Study of Evolution,* 62 (2), 413-420.

Angilletta, Jr., M.J., Niewiarowski, P.H., Dunham, A.E., Leache, A.D. and Porter, W.P. (2004) Bergmann's Clines in Ectotherms: Illustrating a Life-History Perspective with Sceloporine Lizards. *The American Naturalist,* 164 (4), 168-183.

Arendt, J.D. (2011) Size-fecundity relationships, growth tracjectories, and the temperature-size rule for ectotherms. *Evolution,* 65 (1), 43-51.

Ashton. K.G. (2002) Patterns of within-species body size variation of birds: strong evidence for Bergmann's rule. *Global Ecology and Biogeography,* 11, 505-523.

Ashton, K.G. and Feldmann, C.R. (2003) Bergmann's rule in nonavian reptiles: turtles follow it, lizards and snakes reverse it. *Evolution,* 57 (5), 1151-1163.

Ashton, K.G., Tracy, M.C. and de Queiroz, A. (2000) Is Bergmann's Rule Valid for Mammals? *The American Naturalist,* 156 (4), 390-415.

Atkinson, D. (1994) Temperature and organism size: a biological law for ectotherms? *Advances in Ecological Research,* 25, 1-58.

Bergmann, K. (1847). Ueber die verhaltnisse der warmeokonomie der thiere zu ihrer grosse. *Gottinger Studien*, 3, 595–708.

BirdLife International & NatureServe. (2017). Bird species distribution maps of the world. BirdLife International, Cambridge, United Kingdom and NatureServe, Arlington, United States.

Blackburn, T.M. and Gaston, K.J. (1996) Spatial patterns in the body sizes of birds species in the New World. *Oikos,* 77, 436-446.

Blackburn, T.M. and Hawkins, B.A. (2004) Bergmann's rule and the mammal fauna of northern North America. *Ecography,* 27, 715-724.

Blackburn, T.M., Gaston, K.J. and Loder, N. (1999) Geographic gradients in body size: a clarification of Bergmann's rule. *Diversity and Distributions,* 5, 165-174.

Boyce, M. S. (1978) Climatic variability and body size variation in the muskrats (Ondatra zibethicus) of North America, *Oecologia* 36: 1-20.

Boyce, M. S (1979) Seasonality and patterns of natural selection for life histories, *The American Naturalist*, 114: 569-583.

Cabral, J.S., Valente, L., and Hartig, F. (2017) Mechanistic simulation models in macroecology and biogeography: state-of-art and prospects. *Ecography*, 40, 267-280.

Cardillo, M. (2002) Body Size and Latitudinal Gradients in Regional Diversity of New World Birds. *Global Ecology and Biogeography,* 11 (1), 59-65.

Clauss, M., Dittmann, M.T., Müller, D.W.H., Meloro, C. & Codron, D. (2013) Bergmann′s rule in mammals: a cross-species interspecific pattern. *Oikos*, 122, 1465–1472.

Connolly, S.R., Keither, S.A., Colwell, R.K. and Rahbek, C. (2017) Process, Mechanism, and Modelling in Macroecology. *Trends in Ecology and Evolution,* DOI: dx.doi.org/10.1016/j.tree.2017.08.011

Cooper, N., and A. Purvis (2010). Body size evolution in mammals: complexity in tempo and mode. *American Naturalist* 175:727–738.

Cushman, J.H., Lawton, J.H. and Manly, B.F.J. (1993) Latitudinal patterns in Europe ant assemblages: variation in species richness and body size. *Oecologia,* 95, 30-37.

Cvetkovic, D., Tomasevic, N., Ficetola, G.F., Crnobrnja-Isailovic, J. and Miaud, C. (2009) Bergmann's rule in amphibians: combining demographic and ecological parameters to explain body size variation

among populations in the common toad *Bufo bufo. Journal of Zoolological System Evolution Research,* 47 (2), 171-180.

Diniz-Filho, J.A.F., Bini, L.M., Rodriguez, M.A., Rangel, T.F.L.V.B. and Hawkins, B.A. (2007) Seeing the forest for the trees: partitioning ecological and phylogenetic components of Bergmann's rule in European Carnivora. *Ecography,* 30, 598-608.

F. Dormann, C., M. McPherson, J., B. Araújo, M., Bivand, R., Bolliger, J., Carl, G., G. Davies, R., Hirzel, A., Jetz, W., Daniel Kissling, W. and Kühn, I. (2007) Methods to account for spatial autocorrelation in the analysis of species distributional data: a review. *Ecography*, 30(5), 609-628.

Dutilleul, P., Pelletier, B., and Fyles, J.W. (2008) Modified F-tests for assessing the multiple correlation between one spatial process and several others. Journal of Statistical Planning and Inference, 138, 1402-1415.

Geist, V. (1987) Bergmann's rule is invalid. *Canadian Journal of Zoology,* 65, 1035-1038.

Faurby, S. and Araujo, M.B. (2017) Anthropogenic impacts weaken Bergmann's Rule. Ecography, 40, 683-684.

Faurby, S. and Svenning, J.-C. (2015) Historic and prehistoric human-driven extinctions have reshaped global mammal diversity patterns. Diversity and Distributions, 21, 1155-1166.

Feldman, A. and Mieri, S. (2014) Australian Snakes Do Not Follow Bergmann's Rule. *Evolutionary Biology,* 41, 327-335.

Feldman, A., Sabath, N., Pyron, R. A., Mayrose, I. and Meiri, S. (2016) Body-sizes and diversification rates of lizards, snakes, amphisbaenians and the tuatara. *Global Ecology and Biogeography*, 25: 187-197

Ferguson, S.H. and Lariviere, S. (2008) How Social Behaviour Links Environment and Body Size in Mammalian Carnivores. *The Open Ecology Journal,* 1, 1-7.

Freckleton, R.P., Harvey, P.H. and Pagel, M. (2003) Bergmann's Rule and Body Size in Mammals. *The American Naturalist,* 161 (5), 821-825.

Gaston, K.J. (2000) Global patterns in biodiversity. *Nature*, **405**, 220–7.

Geist, V., (1987) Bergmann's rule is invalid. *Canadian Journal of Zoology*, 65(4), 1035-1038.

Hamilton, T.H. (1961) The adaptive significance of intraspecific trends in wing length and body size among bird species. *Evolution,* 15, 180-195.

Harfoot, M.B.J., Newbold, T., Tittensor, D.P., Emmott, S., Hutton, J., Lyutsarev, V., Smith, M.J., Scharlemann, J.P.W., Purves, D.W. (2014) Emergent Patterns of Ecosystem Structure and Function from

a Mechanistic General Ecosystem Model. *PLoS Biology*, 12 (4): e1001841. doi:10.1371/journal.pbio.1001841.

Hawkins, B.A. and Diniz-Filho, J.A. (2006) Beyond Rapoport's rule: evaluating range size patterns of New World birds in a two-dimensional framework. *Global Ecology and Biogeography*, 15, 461-469.

Hijmans, R.J., S.E. Cameron, J.L. Parra, P.G. Jones and A. Jarvis (2005) Very high resolution interpolated climate surfaces for global land areas, *International Journal of Climatology*, 25, 1965-1978.

Ho, C-K., Pennings, S.C. and Carefoot, T.H. (2010) Is diet quality an overlooked mechanism for Bergmann's rule? *American Naturalist*, 175, 269-276.

Hurlbert, A.H. & Jetz, W. (2007) Species richness, hotspots, and the scale dependence of range maps in ecology and conservation. Proceedings of the National Academy of Sciences, 104, 13384–13389.

Huston, M.A. and Wolverton, S. (2011) Regulation of animal size by eNPP, Bergmann's rule, and related phenomena. *Ecological Monographs*, 81 (3), 349-405.

IUCN. (2017). Red List of threatened species v 17.3, <http://www.iucnredlist.org>. Downloaded in December 2017.

James, F.C. (1970) Geographic Size Variation in Birds and Its Relationship to Climate. *Ecology*, 51 (3), 365-390.

Kearney, M., Shine, R., and Porter, W. P. (2009). The potential for behavioral thermoregulation to buffer ''cold-blooded'' animals against climate warming. *Proceedings of the National Academy of Sciences*, 106(10), 3835–3840.

Lindsay, C.C (1966) Body sizes of poikilotherm vertebrates at different latitudes. *Evolution*, 20, 456-465.

Lukin, E.I. (1940) *Darvinizm i geograficheskie zakonomernosti v izmenenii organizmov* (Darwinism and Role of Geographical Patterns of Changes in Organisms), Moscow: Akad. Nauk

Marquet, P.A., Allen, A.P., Brown, J.H., Dunne, J.A., Enquist, B.J., Gillooly, J.F., Gowaty, P.A., Green, J.L., Harte, J., Hubbell, S.P. and O'dwyer, J. (2014) On theory in ecology. *BioScience*, 64(8), pp.701-710.

Martinez, P.A., Marti, D.A., Molina, W.F. and Bidau, C.J. (2013) Bergmann's rule across the equator: a case study in *Cerdocyon thous* (Canidae). *Journal of Animal Ecology*, doi: 10.1111/1365-2656.12076.

Mayr, E. (1956) Geographical character gradients and climatic adaptation. *Evolution*, 10, 105-108.

McNab, B.K. (1971) On the ecological significance of Bergmann's rule. *Ecology*, 52, 845-854.

McNab, B.K. (2010) Geographic and temporal correlations of mammalian size reconsidered: a resource rule. *Oecologia*, 164, 13-23.

Medina, A.I., Martí, D.A. and Bidau, C.J. (2007) Subterranean rodents of the genus Ctenomys (Caviomorpha, Ctenomyidae) follow the converse to Bergmann's rule. Journal of Biogeography, 34(8), pp.1439-1454.

Meiri, S. (2011) Bergmann's Rule - what's in a name? *Global Ecology and Biogeography*, 20, 203-207.

Meiri, S. and Dayan, T. (2003) On the validity of Bergmann's rule. *Journal of Biogeography*, 30, 331-351.

Meiri, S., Dayan, T. and Simberloff, D. (2004) Carnivores, biases and Bergmann's rule. *Biological Journal of the Linnean Society*, 81, 579-588.

Meiri, S. and Thomas, G.H. (2007) The geography of body size - challenges of the interspecific approach. *Global Ecology and Biogeography*, 16, 689-693.

Morales-Castilla, I., Rodriguez, M.A. and Hawkins, B.A. (2012a) Deep phylogeny, net primary productivity, and global body size gradient in birds. *Biological Journal of the Linnean Socitey*, 106, 880-892.

Morales-Castilla, I., Olalla-Tárraga, M.Á., Purvis, A., Hawkins, B.A. & Rodríguez, M.Á. (2012b) The imprint of Cenozoic migrations and evolutionary history on the biogeographic gradient of body size in New World mammals. *The American Naturalist*, 180, 246-256.

Mosseau, T.A. (1997) Ectotherms follow the converse to Bergmann's rule. *Evolution*, 51 (2), 630-632.

Olalla-Tarraga, M.A. (2011) *"Nullis in Bergmann"* or the pluralistic approach to ecogeographic rules: a reply to Watt et al. (2010). *Oikos*, 120, 1441-1444.

Olalla-Tarraga, M.A. and Rodriguez, M.A. (2007) Energy and interspecific body size patterns of amphibian faunas in Europe and North America: anurans follow Bergmann's rule, urodeles its converse. *Global Ecology and Biogeography*, 16, 606-617.

Olalla-Tarraga, M.A., Rodriguez, M.A. and Hawkins, B.A. (2006) Broad-scale patterns of body size in squamate reptiles of Europe and North America. *Journal of Biogeography*, 33, 781-793.

Oliveira, B.F., São-Pedro, V.A., Santos-Barrera, G., Penone, C. and Costa, G.C. (2017) AmphiBIO, a global database for amphibian ecological traits. Scientific Data, 4, p.sdata2017123.

Olson, V.A., Davies, R.G., Orme, D.L., Thomas, G.H., Meiri, S., Blackburn, T.M., Gaston, K.J., Owens, I.P.F. and Bennett, P.M. (2009) Global biogeography and ecology of body size in birds. *Ecology Letters*, 12, 249-259.

Pincheria-Donoso, D., Hodgson, D.J. and Tregenza, T. (2008) The evolution of body size under environmental gradients in ectotherms: why should Bergmann's rule apply to lizards? *BMC Evolutionary Biology*, 8:68 doi:10.1186/1471-2148-8-68

Pincheria-Donoso, D. (2010) The balance between predictions and evidence and the search for universal macroecological patterns: taking Bergmann's rule back to its endothermic origin. *Theory of Bioscience*, 129, 247-253.

Pincheria-Donoso, D. and Mieri, S. (2013) An Intercontinental Analysis of Climate-Driven Body Size Clines in Reptiles: No Support for Patterns, No Signals of Processes. *Evolutionary Biology*, 40, 562-578.

Porter, W.P. and Kearney, M. (2009) Size, shape, and the thermal niche of endotherms, *Proceedings of the National Academy of Sciences*, 106, 19666-19672.

Purves, D., Scharlemann, J., Harfoot, M., Newbold, T., Tittensor, D.P., Hutton, J., Emmott, S. (2013) Time to model all life on Earth. *Nature*, 493, 295-297.

Ramirez, L., Diniz-Filho, J.A.F. and Hawkins, B.A. (2008) Partitioning phylogenetic and adaptive components of the geographical body-size pattern of New World birds. *Global Ecology and Biogeography*, 17, 100-110.

Rapacciuolo, G., Marin, J., Costa, G.C., Helmus, M.R., Behm, J.E., Brooks, T.M., Hedges, S.B., Radeloff, V.C., Young, B.E. and Graham, C.H. (2017) The signature of human pressure history on the biogeography of body mass in tetrapods. *Global Ecology and Biogeography*, 26(9), pp.1022-1034.

Rensch, B. (1938) Some problems of geographical variation and species-formation. *Proceeds of the Linnean Society of London*, 150, 275-285.

Rodriguez, M.A., Lopez-Sanudo, I.L. and Hawkins, B.A. (2006) The geographic distribution of mammal body size in Europe. *Global Ecology and Biogeography*, 15, 173-181.

Rodriguez, M.A., Olalla-Tarraga, M.A., and Hawkins, B.A. (2008) Bergmann's rule and the geography of mammal body size in the Western Hemisphere. *Global Ecology and Biogeography*, 17, 274-283.

Roll, U., Feldman, A., Novosolov, M., Allison, A., Bauer, A.M., Bernard, R., Böhm, M., Castro-Herrera, F., Chirio, L., Collen, B. and Colli, G.R. (2017). The global distribution of tetrapods reveals a need for targeted reptile conservation. *Nature Ecology & Evolution*, 1(11), p.1677.

Rosenzweig, M.L (1968) The strategy of body size in mammalian carnivores. *American Midland Naturalist*, 80, 299-315.

Santini, L., Benítez-López, A., Ficetola, G.F. and Huijbregts, M.A.J. (2017a) Length–Mass allometries in Amphibians. Integrative Zoology.

Santini, L., González-Suárez, M., Rondinini, C. and Di Marco, M. (2017b) Shifting baseline in macroecology? Unravelling the influence of human impact on mammalian body mass. Diversity and Distributions, 23(6), 640-649.

Slavenko, A., Tallowin, O.J., Itescu, Y., Raia, P. and Meiri, S. (2016) Late Quaternary reptile extinctions: size matters, insularity dominates. Global Ecology and Biogeography, 25(11), 1308-1320.

Slavenko, A., Feldman, A., Allison, A., Bauer, A.M., Böhm, M., Chirio, L., Colli, G.R., Das, I., Doan, T.M., LeBreton, M. and Martins, M. (2019) Global patterns of body size evolution in squamate reptiles are not driven by climate. *Global Ecology and Biogeography*, 28(4), pp.471-483.

Smith, M.J., Purves, D.W., Lyutsarev, V. and Emmott, S. (2013) The climate dependence of the terrestrial carbon cycle, including parameter and structural uncertainties. Biogeosciences, 10(1), 583.

Sunday, J.M., Bates, A.E. and Dulvy, N.K. (2010) Global analysis of thermal tolerance and latitude in ectotherms. *Proceedings of the Royal Society B: Biological Sciences*, 278(1713), pp.1823-1830.

Terribile, L.C., Olalla-Tarraga, M.A., Diniz-Filho, J.A.F. and Rodriguez, M.A. (2009) Ecological and evolutionary components of body size: geographic variation of venomous snakes at the global scale. *Biological Journal of the Linnean Society*, 98, 94-109.

Torres-Romero, E.J., Morales-Castilla, I., & Olalla-Tárraga M.Á. (2016) Bergmann´s rule in the oceans? Temperature determines global interspecific patterns of body size in marine mammals. *Global Ecology and Biogeography*, 25: 1206-1215.

Tseng, M. and Soleimani Pari, S. (2019) Body size explains interspecific variation in size–latitude relationships in geographically widespread beetle species. *Ecological entomology*, 44(1), pp.151-156.

Vinarski, M.V. (2014) On the Applicability of Bergmann's Rule to Ectotherms: The State of the Art. *Biology Bulletin Reviews*, 4 (3), 232-242.

Watt, C., Mitchell, S. and Salewski, V. (2010) Bergmann's rule; a concept cluster? *Oikos*, 119, 89-100.

Watt, C. and Salewski, V. (2012) Bergmann's rule encompasses mechanism: a reply to Olalla-Tarraga (2011). *Oikos*, 120, 1445-1447.

Wilman, H., Belmaker, J., Simpson, J., de la Rosa, C., Rivadeneira, M.M. and Jetz, W. (2014) EltonTraits 1.0: Species-level foraging attributes of the world's birds and mammals. Ecology, 95(7), pp.2027-2027.

Wolverton, S., Huston, M.A., Kennedy, J.H, Cagle, K. and Cornelius, J.D (2009) Conformation to Bergmann's Rule in White-tailed Deer can be Explained by Food Availability. *American Midland Naturalist*, 162, 403-417.

DATA ACCESSIBILITY

All modelled body mass data has been deposited in Data Dryad (DOI to be added on acceptance). Empirical data are accessible from the cited sources.

Tables

Table 1. Hypothesised mechanisms contributing to the latitudinal gradients in animal body size.

Mechanism	Description
Chance	Random ancestral colonisation and subsequent diversification may have led to larger body masses at higher latitudes (Blackburn et al., 1999). Alternatively, selective advantages of traits coupled with body mass may cause the pattern.
Migration ability	Smaller species are associated with lower dispersal abilities. The different dispersal velocities of larger and smaller bodied species during the retreat of the late Pleistocene ice sheet therefore results in underrepresentation of smaller species in areas from which ice has retreated (Blackburn and Gaston, 1996; Olalla-Tárraga and Rodríguez, 2007; Morales-Castilla et al., 2012a,b; Martinez et al., 2013).
Predation	Predation risk appears to decrease with distance from the equator. This allows species at high latitude to mature to a larger size *(*Ashton et al., 2000).
Thermoregulation	If animals are the same shape, larger species have increased heat conservation in cooler environments thereby augmenting survival and energy allocation to growth (Bergmann, 1847).
Resource availability	Body mass must be maintained by a sufficient supply of food resources (Rosenzweig, 1968). This supply is governed by net primary productivity (NPP) and competition for resources. Geist (1987) first argued that NPP increases with latitude whilst competition decreases, permitting larger body size at higher latitudes, peaking at 60 - 65° (Wolverton et al., 2009; McNab, 2010; Huston and Wolverton, 2013). Ho et al. (2010) have also asserted that resource quality increases with latitude.
Habitat availability	Larger animals generally need larger habitats. Increased habitat fragmentation in the tropics as a result of concentrated mesoclimate gradients causes unsuitable conditions for larger species (Hawkins and Diniz-Filho, 2006; Rodríguez et al., 2008; Terribile et al., 2009).
Starvation resistance	In regions of great seasonality, larger body mass enhances fasting endurance via the allometric scaling of fat reserves (Geist, 1987; Cushman et al., 1993).

Table 2. Environmental knockout experiments

Label	Experiment
NPP-flat	*Cumulative annual NPP* in each cell was set to the mean cumulative annual productivity across all grid cells, derived from the full model simulations. However, this cumulative total was distributed across months in the same proportions as the productivity calculated by the full model.
NPP-aseasonal	*Seasonality of NPP* in each cell was removed by setting the productivity in each month of the year equal to the annual mean productivity of that cell.
T-flat	*Annual mean temperature* in each cell was set equal to the global annual mean temperature. However, over the course of the model year the temperature in each cell varied around this global with the same absolute deviations as for the original climatological temperatures.
T-aseasonal	*Seasonality of temperature* in each cell was removed by setting the temperature in each month of the year equal to the annual mean temperature of that cell. We also set the diurnal temperature range in each month of the year equal to the annual mean diurnal temperature of that cell.

Figures

Figure 1. Global distributions (a-c) and latitudinal profiles (d-f) of annual mean, community median body masses of endotherms predicted by the Madingley model (a, d), Holocene mammals estimated from empirical data (b, e), present-day birds estimated from empirical data (c, f).

Figure 2. The relative effect on community mean endotherm and ectotherm body mass across latitudes of removing spatial variation in cumulative annual primary production, seasonality of primary production, annual mean temperature and annual temperature seasonality. Solid bars represent the median and grey lines the interquartile range across longitudes with each latitude band. Lighter hue indicates negative median effect whilst darker indicates a positive median effect

Figure 3. Effect of environmental knockouts in a grid cell centred at 62.5°N and 82.5°E on (a) endotherm community size distribution, (b) probability of assimilating biomass, p(A), and of reproducing offspring, p(R), within a year, (c) annual mass assimilated, (d) number of offspring produced per individual present at the start of the year, and proportion of individuals present at the start of the year that die from predation (e) or starvation (f) events. The community size distribution is the annual median abundance per mass bin from the 20th year of the simulation, dashed lines indicate the community mean body mass for each knockout. Points in b – f represent median predicted values from models fitted to annual data from the last 5 years of a 20 year simulation, error bars represent maximum and minimum value across years.

Figure 4. Effect of environmental knockouts in a grid cell centred at 62.5°N and 82.5°E on (a) ectotherm community size distribution, (b) probability of assimilating biomass, p(A), and of reproducing offspring, p(R), within a year, (c) annual mass assimilated, (d) number of offspring produced per individual present at the start of the year, and proportion of individuals present at the start of the year that die from predation (e) or starvation (f) events. The community size distribution is the annual median abundance per mass bin from the 20th year of the simulation, dashed lines indicate the community mean body mass for each

knockout. Points in b – f represent median predicted values from models fitted to annual data from the last 5 years of a 20 year simulation, error bars represent maximum and minimum value across years.